Study of the Optimum Dose of Ferromagnetic Nanoparticles Suitable for Cancer Therapy Using MFH

M. Pavel[1,2], G. Gradinariu[1,2], and A. Stancu[1]

[1]Physics Department, Alexandru Ioan Cuza University, Iasi 700506, Romania
[2]Gr. T. Popa University of Medicine and Pharmacy , Iasi 700115, Romania

At present, a successful realization of the magnetic fluid hyperthermia (MFH) therapy is conditioned by some unsolved problems. One of these problems is the choice of the correct particle concentration in order to achieve a defined temperature increase in the tumor tissue. A computer-based model was created using COMSOL: Multiphysics in order to simulate the heat dissipation within the tissue for typical configurations of the tumor position in relation to neighboring blood vessels as well as particle distribution within the tumor. The temperature achieved on the tumor border was investigated taking into account physiological parameters of different types of tissues. Using the correct nanoparticle dosage and considering their specific loss power, it is possible to estimate the efficiency of this therapeutic method. If the tumor shape and position are known by suitable medical imaging techniques (e.g., MRI, CT), simulations like this one could provide data in order to achieve the optimum dose and particle distribution in the tumor.

Index Terms—**Hyperthermia, magnetic nanoparticles dose, perfusion rate, tumor.**

I. Introduction

MAGNETIC fluid hyperthermia (MFH) represents one of the focal points in the research for an effective cancer therapy due to the promising heating capabilities of ferromagnetic nanoparticles and the advances in the specific delivery of these particles to the tumor. The method consists of inducing apoptosis to the cancer cells by generating heat locally from ferromagnetic or ferrimagnetic nanoparticles which are irradiated with an alternating electromagnetic field. The most commonly used materials are magnetite Fe_3O_4 and maghemite γ-Fe_2O_3, which due to their magnetic properties, low toxicity and good biocompatibility offer many efficient possibilities in biotechnology and medicine [1]–[3]. However, there are still numerous difficulties that need to be overcome before an operating clinical model can be developed. These difficulties include the need to choose biocompatible values for field amplitude and frequency, the problem of quantifying the optimum dose of nanoparticles in order to limit the heating area to the tumor as precise as possible.

The generated heat within the tissue can be attributed to three types of loss processes [2], [4]: hysteresis losses, which correspond to the ferromagnetic (FM) behavior of the particle, relaxation losses which account for most of the generated heat in the superparamagnetic (SPM) regime, and resonance losses which would only occur at high frequencies unsuitable for the MFH therapy and can thus be neglected. In the first case, the hysteresis losses ($\mathrm{LP_{FM}}$ = loss power for FM particles) are equal to the area of the hysteresis loop multiplied by the frequency [1], [5]

$$\mathrm{LP_{FM}} = \mu_0 f \oint \mathrm{HdM} \tag{1}$$

where permeability $\mu_0 = 4\pi \cdot 10^{-7}$ H/m.

In particles with a superparamagnetic behavior, losses may occur either through Brownian or Néel relaxations [3], [4]. The loss power (LP) due to relaxation losses ($\mathrm{LP_{SPM}} = \mathrm{LP}$ for SPM particles) may thus be expressed as [4], [6], [7]

$$\mathrm{LP_{SPM}} = \mu_0 \pi \chi_0 f \frac{2\pi f \tau_R}{1 + (2\pi f \tau_R)^2} H^2 \tag{2}$$

where τ_R is the effective relaxation time, $\chi_0 = \mu_0 M_S^2 V/(\mathrm{kT}), \mathrm{M_S}$ is the saturation magnetization, and V is the particle volume [4], [6]–[8].

In order to successfully induce apoptosis in the cancer cells, enough heat must be generated so that a constant local temperature of 42–46°C is maintained for at least 30 min [1], [6]. The estimation of the actual quantity of heat can be further complicated by the presence of capillaries or other blood vessels that constantly perfuse the tumor. Furthermore, high frequencies (f) and field amplitudes (H) can produce unnecessary heating which can lead to lesions of the surrounding healthy tissue via eddy currents [8], and thus, the parameters of the alternating magnetic field must be rightfully chosen. Brezovich [9] established a criterion of exposure that is safe and tolerable of $\mathrm{H \cdot f} \leq 4.85 \times 10^8\ \mathrm{Am^{-1}s^{-1}}$, which has also been confirmed by Pankhurst [1]. However, considering the main goal of MFH therapy, which is the ablation of the whole tumor, Hergt [10] assumed a weaker criterion of $\mathrm{C} = 5 \times 10^9\ \mathrm{Am^{-1}s^{-1}}$, where $\mathrm{H \cdot f} < \mathrm{C}$. Therefore, by using this criterion in (2), the maximum theoretical value for LP is [10]

$$\mathrm{LP_{SPM-max}} = \mu_0 \pi \chi_0 C^2 \tau_R / \left[1 + \left(C^2 \tau_R^2 / H^2\right)\right]. \tag{3}$$

II. Computer-Based Model

Taking into account the biocompatibility criterion mentioned above and by using formulas (1) and (2), we have calculated the amount of loss power for magnetite and maghemite particles for both superparamagnetic and blocked (particles showing hysteresis) particles. For the superparamagnetic regime, the optimum loss power for therapy was obtained for magnetite for frequencies between 500 and 550 kHz using a field amplitude H of 6.5 kA/m and particle radius of 9–10 nm. By increasing the value of H, we must also balance the frequency by decreasing it. Therefore, considering $\mathrm{H} = 13.5$ kA/m, frequencies range between 160 and 180 kHz, and for the maximum biocompatible value of $\mathrm{H} = 20$ kA/m, the frequency must be less than 90 kHz.

In the ferromagnetic regime, the biocompatible values of H and f are less than 20 kA/m and 600 kHz, respectively [1],

Digital Object Identifier 10.1109/TMAG.2008.2001661

Color versions of one or more of the figures in this paper are available online at http://ieeexplore.org.

[2], [10]. However, the LP due to hysteresis losses for maximum biocompatible values is lower than the LP in the superparamagnetic regime, comparable with the one obtained in the superparamagnetic model for frequencies less than 250 kHz, when $\mathrm{H} = 6.5$ kA/m. All these results are in agreement with other experimental results from Hergt [2], [10] or Pankhurst [1]. We have simulated the heat dissipation generated by magnetic nanoparticles with a given concentration for various types of tissues. In order to estimate the temperature increase within the tissue for *in vivo* conditions we solved in COMSOL the Pennes bioheat transfer equation given by [11] and [12]

$$\delta_{tz}\rho c\frac{\partial T}{\partial t} + \nabla\cdot(-k\nabla T) = \rho_b c_b \omega_b (T_b - T) + Q_{\mathrm{met}} + Q_{\mathrm{ext}}, \quad (4)$$

where ρ is the tissue density, c is the tissue specific heat, ρ_{b} is the density of blood, 1000 kg/m^3, $\mathrm{c_b}$ is the blood' specific heat, 4180 J/(kg $\cdot$ K), k is the tissue thermal conductivity, 0.512 W/(m $\cdot$ K), ω_{b} is the blood perfusion rate, $\mathrm{T_b}$ is the arterial blood temperature, 310.15 K [11], [12], $\mathrm{Q_{met}}$ is the metabolic heat source, which for skin is 400 W/m^3, for glandular tissue is 700 W/m^3, and for cancerous tissue is 5790 W/m^3 [13].

Furthermore, we took into account the existence of blood vessels for all our models which will naturally have the constant systemic temperature due to the high perfusion rate, as may be observed in all figures shown.

Our simulations are based on another model [14] that we designed using the COMSOL (Multiphysics—Heat Transfer Module): the tumor volume is randomly injected in different regions with the same quantity of nanoparticles which are homogenously distributed in order to obtain a fixed concentration. For each of the two nanoparticles behaviors, hysteretic and superparamagnetic, the heat dissipation in the tumor was studied for nanoparticles concentrated in regions of various sizes. In the case of hysteretic behavior, for a given concentration of magnetic material of 12 mg/cm^3, the nanoparticles were equally distributed in 20 spherical regions of 0.6 mm in diameter and six regions with a diameter of 0.9 mm [14]. Using the same values for f and H, considering the loss power of one spherical region of being 5×10^9 W/m^3, in the first simulation, the optimal heating region was obtained at the temperature of 42–42.5°C for 2–3 mm around the particles in the first simulation, and for 4–6 mm in the second distribution. In the superparamagnetic model, for a lower concentration (10.5 mg/cm^3), we considered a number of 18 spherical regions with a diameter of 0.6 mm, respectively, nine spherical regions with a diameter of 0.762 mm, and a loss power of 1×10^8 W/m^3 for each of them, and we obtained a temperature range of 42–42.5°C at 5 to 6 mm distance from the regions and 8 to 10 mm, respectively. We observed that the optimal heating zones (42–43°C) are larger for a denser distribution of nanoparticles within the tissue, when more particles are closer together, for the same concentration and same conditions—field amplitude and field frequency [14].

Using the above results, we studied the reactions of different types of cancerous tissues when MFH therapy is used. We designed distinct simulations of a spherical tumor located in a cubical region of volume 1 cm^3 from the tissue we intended to analyze. For therapeutic LP values, we have chosen a range between (3.4–6.3) $\times 10^9$ W/m^3, as we mentioned above.

In the first simulation, based on the model mentioned above, our next attempt was to estimate a spatial temperature distribution in a tumor of the liver tissue, using magnetite and maghemite nanoparticles in order to compare their therapeutic benefits. Thus, in the second model, we focused on this comparison, and we have used less homogeneity for the particles distribution. The nanoparticles were randomly concentrated in six regions of 0.9 mm diameter each inside the tumor region.

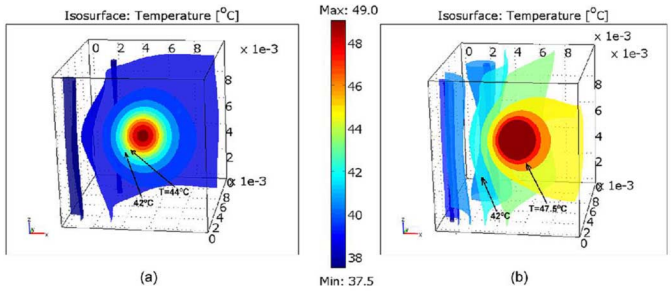

Fig. 1. Spatial temperature distribution in a (a) breast tissue tumor and (b) skin tissue tumor; $\mathrm{LP} = 4.15 \times 10^9$ W/m^3 ($\mathrm{H} = 7$ kA/m, $\mathrm{f} = 260$ kHz, concentration of 10 mg/cm^3, $\mathrm{particle\ diameter} = 18$ nm), T is the tumor border temperature.

TABLE I
PHYSICAL AND PHYSIOLOGICAL PROPERTIES

Type of Tissue	Tumor Density (mg/cm³)	Tissue Density (mg/cm³)	Tumor perfusion rate (1/s)	Tissue perfusion rate (1/s)	Specific heat (J/kg·K)
Breast	1060[12]	980[15]	0.01333[13]	0.00667[13]	2300[16]
Brain	1060[12]	1040[17]	0.01392[18]	0.005[16]	3650[16]
Liver	1160[12]	1040[16]	0.0064[12]	0.0064[12]	3600[12]
Skin	1160[12]	1050[17]	0.0135[18]	0.00833[16]	1730[16]

Concluding the benefits of magnetite magnetic material, we advanced further our simulations. For the second model, we have considered the existence of two small blood vessels (of 0.1 mm in diameter) positioned at approximately 2.5 mm and 4 mm away from the tumor region of 2.7–2.8 mm in diameter. We considered for comparison two different cases. In the first one, we supposed that the magnetite nanoparticles are homogenously distributed in various types of cancerous tissues. We simulated the heat dissipation for brain, breast, liver, and skin tissues taking into account their respective physical and physiological properties (tumor/healthy tissue perfusion rate and density). The values for the biological constants were obtained for each type of tissue from various sources (see Table I). In Fig. 1, this distribution may be seen for breast and skin tissue.

For the second one, we have used less homogeneity for the particles distribution. The nanoparticles were randomly concentrated in six regions of 0.9 mm diameter each inside the tumor region. In both cases, the concentration of magnetic material was varied from 6 up to 15 mg/m^3.

Furthermore, for establishing the importance of the blood vessels' presence near the tumor region, we have chosen for analyzing the liver tissue. By considering only one blood vessel situated at 4 mm distance from the tumor border, we compared the temperature at different points situated between the tumor border and 1.6 mm away from it. For the next simulation, we assumed the presence of a single blood vessel with a diameter of 0.1 mm, positioned 3.5–4 mm away from the tumor. Thirdly, we reduced even more the nanoparticles distribution homogeneity, considering that the magnetic particles are distributed in nine spherical regions ($\mathrm{diameter} = 0.762$ mm) randomly disposed within the tumor volume. For different magnetic material concentrations and LP values, we aimed to compare the influence of a larger tumor volume (18 mm^3—approximately 3 mm $\times$ 3 mm $\times$ 2 mm and 30 mm^3, respectively 4 mm $\times$ 3 mm $\times$ 2.5 mm).

TABLE II
TUMOR BORDER TEMPERATURE

Material	Tumor Diameter (mm)	Particle Concentration (mg/cm³)	Border Temperature (ºC)
Magnetite	3.2	10	49.5
	4.6	3.36	45.8
	6	1.5	42
Maghemite	3.2	10	46
	4.9	3.1	45.6
	8.9	0.5	42

Particle concentrations and border temperature for different sizes of tumors using magnetite or maghemite particles; conditions: H=6.5kA/m, f=300kHz magnetite nanoparticles diameter=18nm and maghemite nanoparticles diameter=22nm.

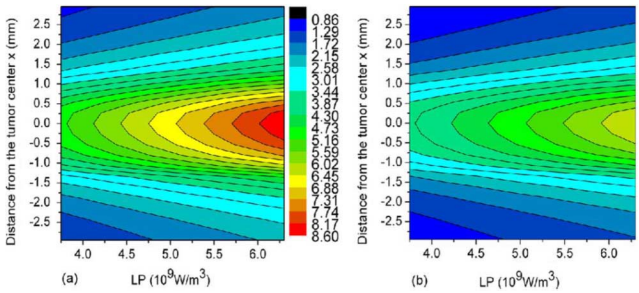

Fig. 2. Temperature differences (°C) in the piece of liver tissue considered when two concentrations are used. (a) 10 mg/cm^3 and 6 mg/cm^3. (b) 13 mg/cm^3 and 10 mg/cm^3.

III. RESULTS

The first simulation shows the heat dissipation that takes place in a liver tumor surrounded by healthy liver tissue. We used a field amplitude H of 6.5 kA/m and a frequency f of 300 kHz. The particle diameter was chosen 18 nm for magnetite and 22 nm for maghemite, respectively, so that we can study the losses in the superparamagnetic regime. In Table II, the differences between the heating capabilities of the two magnetic materials used are shown. Although maghemite nanoparticles may be seem more effective at lower concentrations (see Table II), we concluded by simulations that they are more difficult to work with, considering the fact that for a particle diameter larger than 23 nm or smaller than 21 nm the amount of heat generated within the tissue is either too high or too low for efficient MFH therapy.

In the next simulation, we were interested in obtaining a temperature higher than 42.5°C, the minimum temperature that can induce apoptosis in cancerous tissues. For liver and breast tissue, we observed an almost linear increasing of temperature with concentration and LP. For skin and brain tissue, the presence of the two vessels have a great influence on heat dissipation. In the case of brain cancerous cells, the ideal tumor temperature is obtained choosing values for H and f in order to achieve a LP value around (4.2–4.8) $\times$ 10^9 W/m^3 for a concentration of magnetic nanoparticles of 10 mg/cm^3. In the case of epidermis cancerous regions, the optimum temperature is obtained for a lower concentration (6 mg/cm^3), demonstrating a tumor border temperature higher than the ones obtained in the other types of tissues with 4–5°C in the same conditions. All these aspects may be seen in Figs. 2 and 3.

In Table III are shown the temperatures achieved at tumor border and, respectively, at 0.4 mm and 0.8 mm distance from it using a concentration of nanoparticles of 10 mg/cm^3 and LP values of (3.75–4.5) $\times$ 10^9 W/m^3.

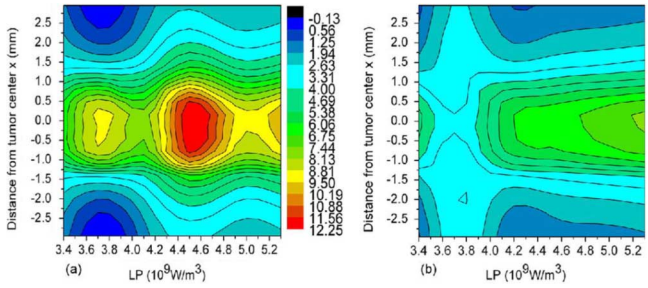

Fig. 3. Temperature differences (°C) in the piece of brain tissue considered when two concentrations are used. (a) 10 mg/cm^3 and 6 mg/cm^3. (b) 13 mg/cm^3 and 10 mg/cm^3.

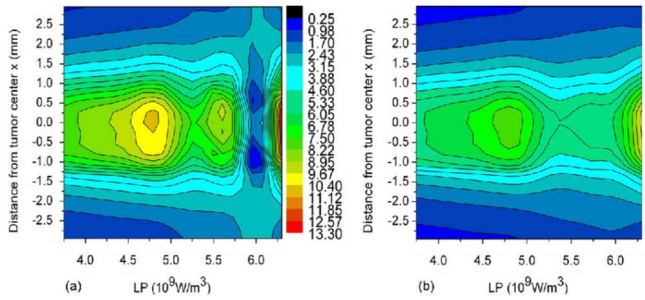

Fig. 4. Temperature differences (°C) in the piece of skin tissue considered when two concentrations are used. (a) 10 mg/cm^3 and 6 mg/cm^3. (b) 13 mg/cm^3 and 10 mg/cm^3.

TABLE III
TEMPERATURE IN DIFFERENT TYPES OF TISSUES

Type of tissue	Tumor Diameter (mm)	Tumor Border Temperature (ºC)	Temperature (ºC) (x = 0.4mm)	Temperature (ºC) (x = 0.8mm)
Breast	3.75	48.638	45.389	43.233
	4.5	50.966	47.066	44.479
	4.9	52.207	47.962	45.145
Brain	3.75	45.559	42.872	41.155
	4.5	47.681	45.254	43.604
	4.9	48.639	45.987	44.191
Liver	3.75	43.344	41.966	41.04
	4.5	44.613	43.7	41.848
	4.9	44.994	43.489	42.279
Skin	3.75	45.555	43.062	41.155
	4.5	47.271	44.047	41.986
	4.9	48.184	46.227	42.429

Temperatures at different distances from tumor border at a concentration of magnetite nanoparticles of 10mg/cm³ with a diameter of 18nm and LP of 4.15×10^{9}W/m³ in superparamagnetic regime.

For liver tissues, we studied the density of larger blood vessels' influence. We compared the results mentioned above with the ones achieved when modeling only one arterial blood vessel (at approximately 4 mm away from the tumor region). We observed that for concentration smaller than 10 mg/cm^3, the dependence of temperature with concentration and LP may not be easily estimated because of the multiple fluctuations. By enlarging the tumor diameter (3.5–4 mm), in the conditions of lower nanoparticles concentrations of 4 to 5 mg/cm^3 and by using the same values for LP (respectively, the same H, f, particle size), we obtained a temperature of 42.5–43.5°C at the interface between tumor and healthy tissue.

For the third model, we also have used liver tissue because liver tumors are known to be difficult to treat surgically. Considering a tumor volume of 18 mm^3 (approximately 3 mm $\times$ 3 mm $\times$ 2 mm), in the superparamagnetic regime, and taking LP = 1.17 $\times$ 10^{10} W/m^3 (H = 7.5 kA/m for a frequency of 250 kHz)

TABLE IV
TUMOR BORDER TEMPERATURE

Magnetite Concentration (mg/cm^3)	LP (W/m^3)$\times 10^9$	Temperature (°C)
10	6	42.195
10	10	45.659
13	6	43.454
13	10	48.257
16	6	45.312
16	10	50.854

Tumor border temperature in liver tissue for magnetite nanoparticles of 18nm in superparamagnetic regime.

and a fixed concentration ranging from 10 mg/cm^3 to 5 mg/cm^3, the temperature around the cancerous tissue was 46.19°C and 41.7°C, respectively. In the ferromagnetic model, for the same value of field amplitude, with the field frequency of 300 kHz and a concentration of 15 mg/cm^3, the temperature around the tumor region was 41.3°C. Thus, in order to obtain the minimum optimal therapeutic value for the temperature (42°C), at least a field amplitude value of $\mathrm{H} = 14.5$ kA/m and a frequency of $\mathrm{f} = 410$ kHz at a dosage of 10 mg/cm^3 are needed (LP higher than 6×10^9 W/m^3). Values of tumor border depending on concentration and LP are shown in Table IV.

We could also obtain the optimum temperature for an increased tumor volume of 30 mm^3 (approximately 4 mm $\times$ 3 mm $\times$ 2.5 mm) for a lower frequency of 170 kHz by using a concentration of 10 mg/cm^3.

IV. DISCUSSIONS

Our results from the first model show that a more effective MFH therapy is obtained by using magnetic instead of maghemite nanoparticles.

Secondly, we observed that in comparison with the other analyzed tumor tissues, therapy of the skin tumors has two main advantages: they can be easily manipulated by means of direct injection and also need a very low concentration for successful hyperthermia treatment (as may be observed from Fig. 4 and Table III). Moreover, breast tumors could be ablated using MFH, mainly due to the lower tissue perfusion rate and to the lower concentration of nanoparticles necessary to generate the optimal temperature of 42.5°C.

Finally, the results for the last simulation show that in the superparamagnetic behavior, the concentration of the particles is much more significant in determining the amount of generated heat, as opposed to the parameters of field amplitude and frequency. However, the practical problem that arises is related to the control of the exact dose of particles in all the cancerous regions. In the case of the ferromagnetic behavior, we observed that the field amplitude and frequency must be significantly increased in order to obtain the same size for the optimum temperature region for the same concentration of nanoparticles as in the superparamagnetic regime.

V. CONCLUSION

In conclusion, our results show that by using these models, we can successfully estimate the impact of the particle dose on the efficiency of hyperthermia therapy, also taking into account the local features (e.g., tumor density, type, and perfusion rate) and external factors (e.g., field amplitude and frequency) involved. It could be thus a good method to evaluate the prospects of the therapy for a given patient who has a well-described condition and also to establish an optimum starting dose for MFH therapy in such a case.

ACKNOWLEDGMENT

This work was supported by the Romanian PNII-26 NANOPART project.

REFERENCES

[1] Q. A. Pankhurst, J. Connolly, S. K. Jones, and J. Dobson, "Applications of magnetic nanoparticles in biomedicine," *J. Phys. D: Appl. Phys.*, vol. 36, pp. R167–R181, 2003.
[2] R. Hergt, W. Andra, C. G. d'Ambly, I. Hilger, W. A. Kaiser, U. Richter, and H. G. Schmidt, "Physical limits of hyperthermia using magnetite fine particles," *IEEE Trans. Magn.*, vol. 34, pp. 3745–3754, 1998.
[3] M. Ma, Y. Wu, H. Zhou, Y. K. Sun, Y. Zhang, and N. Gu, "Size dependence of specific power absorption of Fe3O4 particles in AC magnetic field," *J. Magn. Magn. Mater.*, vol. 268, pp. 33–39, 2004.
[4] L. Y. Zhang, H. C. Gu, and X. M. Wang, "Magnetite ferrofluid with high specific absorption rate for application in hyperthermia," *J. Magn. Magn. Mater.*, vol. 311, pp. 228–233, 2007.
[5] S. Bae, S. W. Lee, Y. Takemura, E. Yamashita, J. Kunisaki, S. Zurn, and C. S. Kim, "Dependence of frequency and magnetic field on self-heating characteristic of NiFe2O4 nanoparticles for hyperthermia," *IEEE Trans. Magn.*, vol. 42, pp. 3566–3568, 2006.
[6] R. Hergt, S. Dutz, R. Muller, and M. Zeisberger, "Magnetic particle hyperthermia: Nanoparticle magnetism and materials development for cancer therapy," *J. Phys: Condens. Matter*, vol. 18, pp. S2919–S2934, 2006.
[7] B. Payet, A. Siblini, M. F. Blanc-Mignon, and G. Noyel, "Comparison between a magneto-optical method and Fannin's technique for the measurement of Brown's relaxation frequency of ferrofluid," *IEEE Trans. Magn.*, vol. 35, pp. 2018–2023, 1999.
[8] R. Hergt, R. Hiergeist, I. Hilger, W. A. Kaiser, Y. Lapatnikov, S. Margel, and U. Richter, "Maghemite nanoparticles with very AC-losses for application in RF-magnetic hyperthermia," *J. Magn. Magn. Mater.*, vol. 270, pp. 345–357, 2004.
[9] I. A. Brezovich and R. F. Meredith, "Practical aspects of ferromagnetic thermoseed hyperthermia," *Radiol. Clin. North. Amer.*, vol. 27, pp. 589–602, 1989.
[10] R. Hergt and S. Dutz, "Magnetic particle hyperthermia- biophysical limitations of a visionary tumour therapy," *J. Magn. Magn. Mater.*, vol. 311, pp. 187–192, 2007.
[11] S. Maenosono and S. Saita, "Theoretical assessment of FePt nanoparticles as heating elements for magnetic hyperthermia," *IEEE Trans. Magn.*, vol. 42, pp. 1638–1642, 2006.
[12] COMSOL Multiphysics, Heat Transfer Module, User's Guide, pp. 145–161, and Model Library, pp. 243-264 .
[13] E. Y. K. Ng and N. M. Sudharsan, "Effect of blood flow, tumor and cold stress in a female breast: A novel time-accurate computer simulation," *J. Biomed. Eng.*, vol. 215, pp. 393–404, 2001.
[14] M. Pavel, G. Gradinariu, and A. Stancu, "A study of the interactions between ferromagnetic nanoparticles used in MFH," IEEE ROMSC 2007. Iasi, Romania, 2007.
[15] J. A. Shepherd, K. M. Kerlikowske, R. Smith-Bindman, H. K. Genant, and S. R. Cummings, "Measurement of breast density with dual x-ray absorptiometry: Feasibility," *Radiology*, vol. 223, pp. 554–557, 2002.
[16] C. Sturesson and S. A. Engels, "A mathematical model for predicting the temperature distribution in laser-induced hyperthermia. Experimental evaluation and applications," *Phys. Med. Biol.*, vol. 40, pp. 2037–2052S, 1995.
[17] C. B. Saw, A. Loper, K. Komanduri, T. Combine, S. F. Huq, and C. Scicutella, "Determination of CT-to-density conversion relationship for image-based treatment planning systems," *Med. Dosim.*, vol. 30, pp. 145–148, 2005.
[18] Z. Rumboldt, R. Al-Okaili, and J. P. Deveikis, "Perfusion CT for head and neck tumors: Pilot study," *Amer. J. Neuroradiol.*, vol. 26, pp. 1178–1185, 2005.

Manuscript received March 02, 2008. Current version published December 17, 2008. Corresponding author: M. Pavel: (e-mail: everblue182004@yahoo.com).